TRANSVERSE PERMEABILITY OF OSB. PART II. MODELING THE EFFECTS OF DENSITY AND CORE FINES CONTENT

Hamid R. Fakhri
Graduate Research Assistant

Kate E. Semple
Postdoctoral Fellow

and

*Gregory D. Smith**
Assistant Professor
Department of Wood Science
University of British Columbia
Vancouver, BC
Canada V6T 1Z4

(Received June 2005)

ABSTRACT

In this work a simple rule of mixtures model to characterize the permeability of an OSB composite as a function of fines contents and density is presented. Strands and fines in the core of the board are considered to lie between two extremes, either stacked in a series configuration (series model) or side by side in a parallel configuration (parallel model), with the permeability of the composite, K_{system}, being a function of relative permeabilities of the series and parallel models. Equations for the permeability of these two configurations, $K_{parallel}$ and K_{series}, are developed as functions of the known permeability of 100% strands, K_s, and 100% fines, K_f, and the mass fraction of fines, M_f. Data on the permeability of the core of OSB compressed to three density classes and made with 0 and 100% fines content are used to determine the permeability of the parallel and series models, respectively. The series coefficient, α, which represents the contribution from the series model, is determined using least squares fits to the permeability data for different target densities and 25%, 50%, and 75% fines contents. α was fairly consistent, ranging from 0.47 to 0.49 for these fines contents. $K_{parallel}$ increases linearly with increasing fines content and K_{series} increases exponentially, in accord with the actual data. The data for the low and medium target density boards were well described by the K_{system} predictions, whereas the model underestimates the permeability of boards containing 75% or 100% fines and compressed to high target density. The model was most sensitive to changes in M_f, K_f, and K_s, with other parameters, α and density ratio (ρ_s/ρ_f), having smaller effects. The proposed model is general and could be applied to other composites of mixed particle sizes such as particleboard.

Keywords: Wood composites, OSB, transverse permeability, fines content, core density, modeling, rule of mixtures.

INTRODUCTION

In Part I of this series, the transverse permeability of OSB made at different target densities and core fines contents was measured. Fines content, target density, and their interaction strongly affected the permeability of the core layer, indicating that there may be benefits not only for increased wood efficiency in plants but potentially improvements in pressing times, particularly for higher density products. In this follow-up report, a model for the permeability of the core of OSB based on an electrical analogy of series and parallel conduction is presented. The effect of fines content in the core is modeled using a rule of mixtures approach from knowl-

* Corresponding author.

edge of the permeability of core layer material made from either 100% strands or 100% fines.

Accurately modeling the processes of heat conduction and convection in a wood composite mat is complicated by the constant changes in permeability and thermal conductivity of the mat both through its thickness and in-plane during compression (Bolton and Humphrey 1988). This is compounded by continuous loss of heat and moisture from the edges of the mat (Strickler 1959; Bowen 1970; Kavvouras 1977). Convection is the primary means of heat transfer during hot-pressing of wood-based composite mats (Strickler 1959; Haas et al. 1998; Bolton and Humphrey 1988). However, early models to calculate the rate of heat flow into particleboard were limited to conduction, and were unable to account for convective heat transfer, energy flux through vapor condensation, and in-plane flow of moisture and heat through the mat (Bolton and Humphrey 1988). A one-dimensional object-oriented finite element pressing model for OSB was developed by Hubert and Dai (1999) to predict transient temperature and internal steam pressure profiles for mats with different initial MC and densities, as modern computing capacity now enables 2D and 3D real-time predictions of temperature and pressure profiles to be predicted in mats during the pressing cycle. A comprehensive mat consolidation model to predict the changes in vertical density profile of OSB during pressing was then subsequently developed (Dai et al. 2000). A hot-pressing model to predict temperature and gas pressure in continuously pressed wood composite mats was developed by Humphrey and Thoemen (2000). A surrogate for mat permeability used in the mass transfer component of their model to calculate the distribution of mat MC and vapor pressure was based solely on mat local density, and did not contain any adjustment for variation in mat structure produced by varying strand size distribution. Nevertheless, for a given fixed mat structure, the predicted trends for core temperature and steam pressure agreed well with measured trends.

Recent, more comprehensive models to simulate the heat and mass transfer conditions of OSB during hot-pressing include Garcia (2002), Zombori et al. (2003), and Dai and Yu (2004). These contain equations for mat specific heat, thermal conductivity, and permeability mat as functions of density. The void fraction of the mat, calculated using a mat formation model developed by Zombori et al. (2001), is used to develop the thermal conductivity and gas permeability components of the model. Garcia (2002) investigated the critical effects of flake alignment on mat permeability and heat and mass transfer. Dai and Yu (2004) use Haas's 1998 density-based model for permeability of OSB mats, but note that information on the relationships between mat permeability and thermal conductivity and wood element geometry are almost completely lacking. Recent work by Dai et al. (2005) helps address this gap with a generalized model to predict OSB mat porosity and permeability in terms of void volume and wood element size. More information on how changing mat structure (i.e. fines content and packing) affects permeability of OSB and a conceptual framework to describe permeability of OSB is still required. The objectives of this study are as follows:

1. Use the permeability data from Part I to develop a model based on rule of mixtures of series and parallel models to describe the effect of fines content on composite transverse permeability.
2. Explore the sensitivity of the model to changing input parameters.

MODEL DEVELOPMENT

The cross-section through the core layer of commercial OSB containing a mixture of strands and fines can be broken down into any number of cells, some of which consist of layers of strands and fines aligned horizontally, i.e. in series, as illustrated in scheme 1 on Fig 1a and b. In other cells, fines may lie adjacent to strands, i.e. parallel to each other with respect to the direction of flow, as shown in scheme 2. Most of the regions through the board cross-section may be characterized by strands and fines arranged in

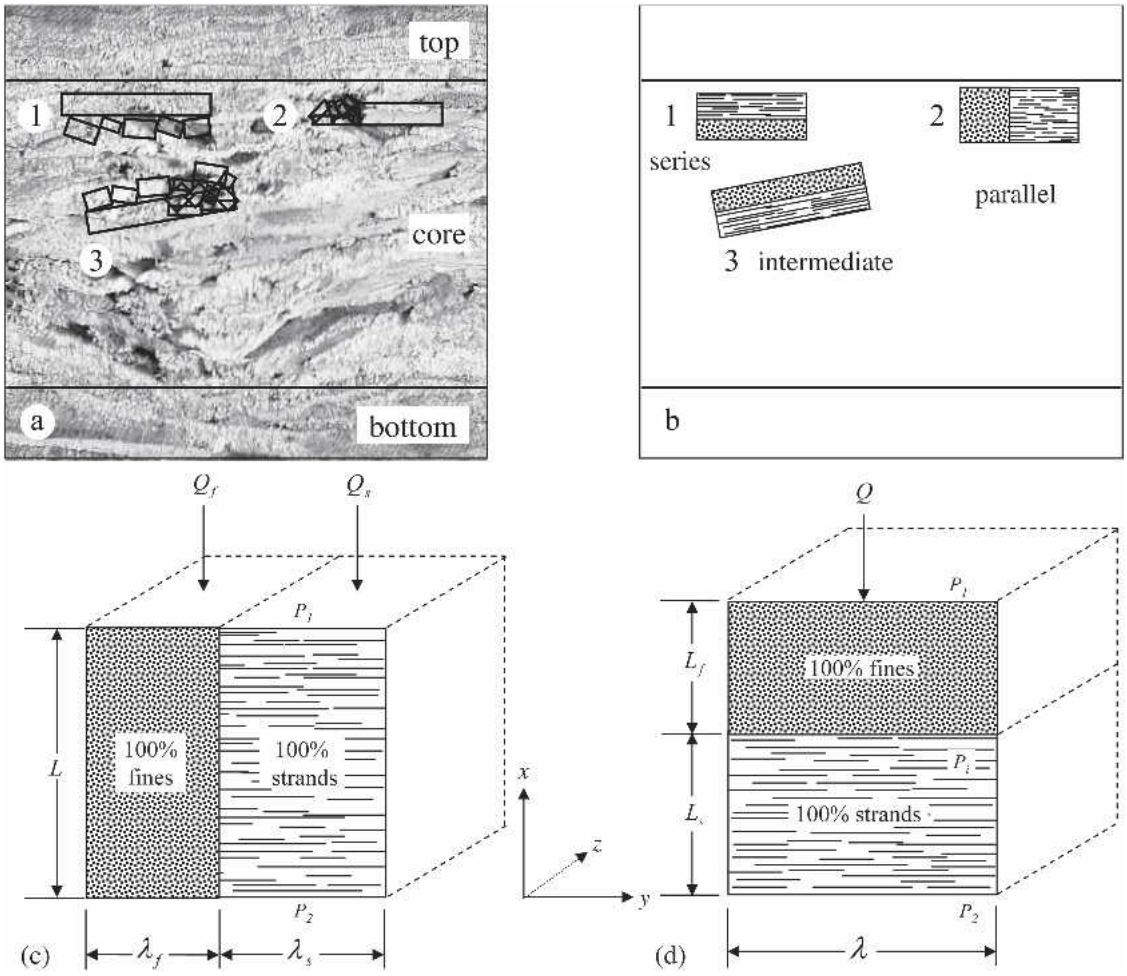

FIG. 1. (*a*) Enlarged scanned cross-section of an OSB sample showing three possible arrangements of strand and fines, (*b*) schematic representation of the three labeled items, (*c*) schematic of parallel model, and (*d*) schematic of series model.

an intermediate configuration between the series and parallel arrangements, as in scheme 3 on Fig. 1a and b. The parallel model is represented in Fig 1c whereby the fines and strands layers are adjacent to each other and gas flows through both components simultaneously. In the series model, represented in Fig. 1d, the gas flows through one layer, then the other layer. The rule of mixtures approach considers the permeability of the OSB core, K_{system}, to be the sum of contributions from the series and parallel models, and it is expected that their relative contributions may be a function of many factors such as fines content, wood element geometry, or compression ratio. This weighting factor is for convenience expressed as the series coefficient, α.

$$K_{system} = \alpha K_{series} + (1 - \alpha) K_{parallel} \qquad (1)$$

Although α may not be constant across different fines contents, this assumption is examined later using the data sets for each fines content.

Parallel model

From Fig. 1c, assuming no horizontal flow, the total transverse flow through the parallel

model is the sum of flows through the strands volume and the fines volume. Applying Darcy's Law:

$$\frac{K_{parallel}A_t\Delta P}{\mu L}=\frac{K_fA_f\Delta P}{\mu L}+\frac{K_sA_s\Delta P}{\mu L} \qquad (2)$$

where $K_{parallel}$ is the permeability of the parallel model, A the cross-sectional area of flow, ΔP is the pressure differential across the sample, L is layer thickness in the flow direction, μ the dynamic viscosity of the fluid (i.e. 1.846×10^{-5} Pa·s for air); the subscript t refers to the total model, f to fines layer and s to the strands layer. The permeability of the parallel configuration may be expressed as a function of the permeability of 100% strands, K_f, and 100% fines, K_s, and the widths of the strands and fines layers, λ_s and λ_f, and so Eq. (2) can be simplified to:

$$k_{parallel}(\lambda_f+\lambda_s)=K_f\lambda_f+K_s\lambda_s$$

$$\text{or} \quad K_{parallel}=\frac{K_f\lambda_f+K_s\lambda_s}{\lambda_f+\lambda_s} \qquad (3)$$

The mass fraction of fines is:

$$M_f=\frac{m_f}{m_f+m_s} \qquad (4)$$

where the mass of fines, m_f, is equal to $\rho_f\lambda_fL$ (which assumes unit depth of the cell = 1), and mass of strands, m_s, is equal to $\rho_s\lambda_sL$; ρ_s and ρ_f are the strand or fines component densities, respectively; A is the cross-sectional area of the strands or fines cell, i.e. λ (1), and L is the thickness in the flow direction, Fig. 1c. Inserting the expressions for m_f and m_s into Eq. (4) and solving for λ_s gives:

$$\lambda_s=\frac{(1-M_f)\rho_f}{M_f\rho_s}\lambda_f \qquad (5)$$

The expression for $K_{parallel}$ is then obtained by substituting Eq. (5) into Eq. (3) to produce:

$$K_{parallel}=\frac{M_fK_f+(1-M_f)K_s\dfrac{\rho_f}{\rho_s}}{M_f+(1-M_f)\dfrac{\rho_f}{\rho_s}} \qquad (6)$$

For convenience, it is assumed that $\rho_s = \rho_f$; the validity of this assumption is assessed in the model sensitivity analysis. Equation (6) then reduces to:

$$K_{parallel}=M_fK_f+(1-M_f)K_s \qquad (7)$$

Series model

Applying Darcy's Law to the two consecutive layers of the series model and noting that P_1 and P_2 are the inlet and outlet pressures, and P_i is the pressure at the interface between the strands and fines layers, then:

$$Q_f=\frac{K_fA(P_1-P_i)}{L_f}, \quad \text{and} \qquad (8)$$

$$Q_s=\frac{K_sA(P_i-P_2)}{L_s} \qquad (9)$$

where L_f and L_s are the thicknesses of the fines and strands layers in the flow direction.

Setting these equations equal to each other and solving for P_i gives:

$$P_i=\frac{P_2+\phi P}{1+\phi} \quad \text{where} \quad \phi=\frac{K_fL_s}{K_sL_f} \qquad (10)$$

In the same manner, the gas flow through the series model is equal to the flow through the fines layer, i.e., $Q = Q_f$. Darcy's equations for Q and Q_f provide an expression for the permeability of the series model:

$$\frac{K_{series}A(P_1-P_2)}{L_f+L_s}=\frac{K_fA(P_1-P_i)}{L_f} \qquad (11)$$

Substituting the expression for P_i, Eq. (10), into Eq. (11) and solving for K_{series} gives:

$$K_{series}=\frac{K_fK_s(L_f+L_s)}{K_sL_f+K_fL_s} \qquad (12)$$

which is only a function of K_f and K_s and thicknesses of the strands and fines layers.

Expressions for L_s and L_f in terms of the mass fraction of fines in the configuration can be obtained by recalling that the mass of the fines layer is given by $m_f = \rho_fL_fA$ and that of the strands layer by $m_s = \rho_sL_sA$, where ρ_f and L_f are the density and thickness of the fines layer, re-

spectively, and ρ_s and L_s are the density and thickness of the strands layer, with A being the cross-sectional area in the flow direction and is the same for both layers.

Substituting the equations for m_f and m_s into Eq. (4), and solving for L_s gives:

$$L_s = \frac{(1 - M_f)\rho_f}{M_f \rho_s} L_f \tag{13}$$

Substituting Eq. (13) into Eq. (12) and simplifying gives:

$$K_{series} = \frac{K_f K_s \left(M_f + (1 - M_f) \dfrac{\rho_f}{\rho_s} \right)}{K_f (1 - M_f) \dfrac{\rho_f}{\rho_s} + M_f K_s} \tag{14}$$

And recalling the assumption that $\rho_s = \rho_f$, Eq. (14) reduces to:

$$K_{series} = \frac{K_f K_s}{K_f (1 - M_f) + M_f K_s} \tag{15}$$

Equations (1), (7), and (14) define the permeability of the core layer of an OSB sample containing any given mixture of fines and strands, K_{system}. The sensitivity of the predicted permeability, K_{system}, to ±15% change in M_f, K_s, K_f, ρ_f/ρ_s, and α by is also examined. The intuitive notion that α may decrease with increasing fines content, i.e the more frequent occurrence of the parallel configuration compared with the series configuration, is also discussed.

RESULTS AND DISCUSSION

The measured permeability and density of core layer samples from Part I containing 100% strands, K_s, or 100% fines, K_f, are shown in Fig. 2. Expressions for permeability as a function of density are obtained from least squares fits of an exponential curve of the form $K_i = ae^{-b\rho}$ for the core samples containing 100% strands, Fig. 2a, and 100% fines, Fig. 2b. The equations of best fit are as follows:

$$K_s = 45{,}937 \times 10^{-13}\, e^{-0.0165\rho} \quad \text{for 100\% fines, and} \tag{16}$$

$$K_f = 1{,}405.2 \times 10^{-13}\, e^{-0.0054\rho} \quad \text{for 100\% strands.} \tag{17}$$

Permeability predictions

By substituting the above equations for K_s and K_f terms into Eqs. (7) and (14), a set of perme-

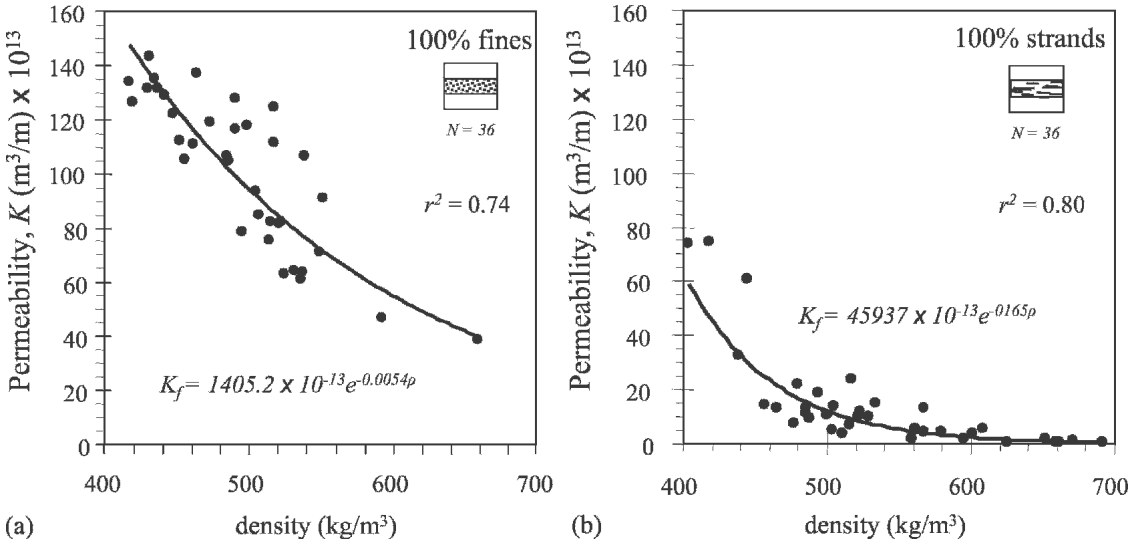

FIG. 2. The permeability of the core layer as a function of density for (*a*) 100% strands, and (*b*) 100% fines. The lines represent least squares fits to the data with their functions shown on each figure.

ability-density curves can be generated for the series and parallel models at different fines contents as shown in Fig. 3a for the parallel model, and 3b for the series model. For a given density, in this case 540 kg/m^3 which is similar to that of commercial OSB, the parallel model shown in Fig. 3a shows a consistent increase in K_{core} with each 25% increment in fines content. In contrast, the increment in permeability of the series model, Fig. 3b, increases exponentially with each 25% increase in fines content. At any given fines content (except 0% and 100%), the permeability of the parallel model is always larger than the series model.

The model predictions for permeability of the system at 25%, 50%, and 75% fines content are shown by the solid lines in Figs. 4a to c, and the predictions of the parallel and series models are shown by the dashed lines above and below, respectively. The parallel and series models generally correspond to the upper and lower bounds of the data, respectively. Note also that as fines content increases the difference between K_{series} and $K_{parallel}$ increases.

Determination of α

As mentioned earlier, the series coefficient α determines the contribution of each model to the overall system permeability. The value of α was determined iteratively using a spreadsheet and its value adjusted until the minimum value of the sum of square errors between the model and the data was found. The system response therefore corresponds to the curve of best fit to the data sets. The optimum value for α was 0.47 at the fines contents of 25% and 50% and 0.49 for the 75% fines content. The solid curves for the system responses at the three fines contents shown in Figs. 4a to c are based on these α values. Interestingly, α appears to be fairly constant from 25% to 75% fines content, and can be given an average value of 0.48.

α *and fines content*

The permeability of the system and the parallel and series models with increasing fines content at 500 kg/m^3 and an $\alpha = 0.48$ are compared in Fig. 5a. Note first that $K_{parallel}$ increases linearly with fines content while K_{series} increases exponentially. K_{series} is always lower than $K_{parallel}$ except at the limits of 100% strands or 100% fines, where by definition $K_{system} = K_{strands}$ or K_{fines}. The roughly equal contributions from the parallel and series models can be seen whereby K_{system} is almost equidistant from both.

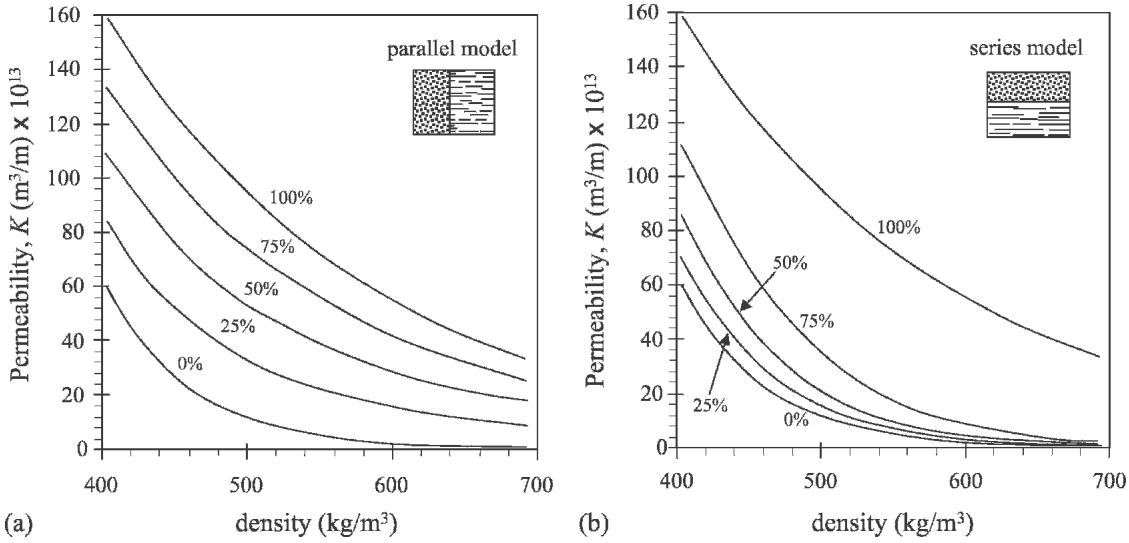

FIG. 3. Predicted permeability as a function of density for different fines contents of (*a*) the parallel model and (*b*) the series model.

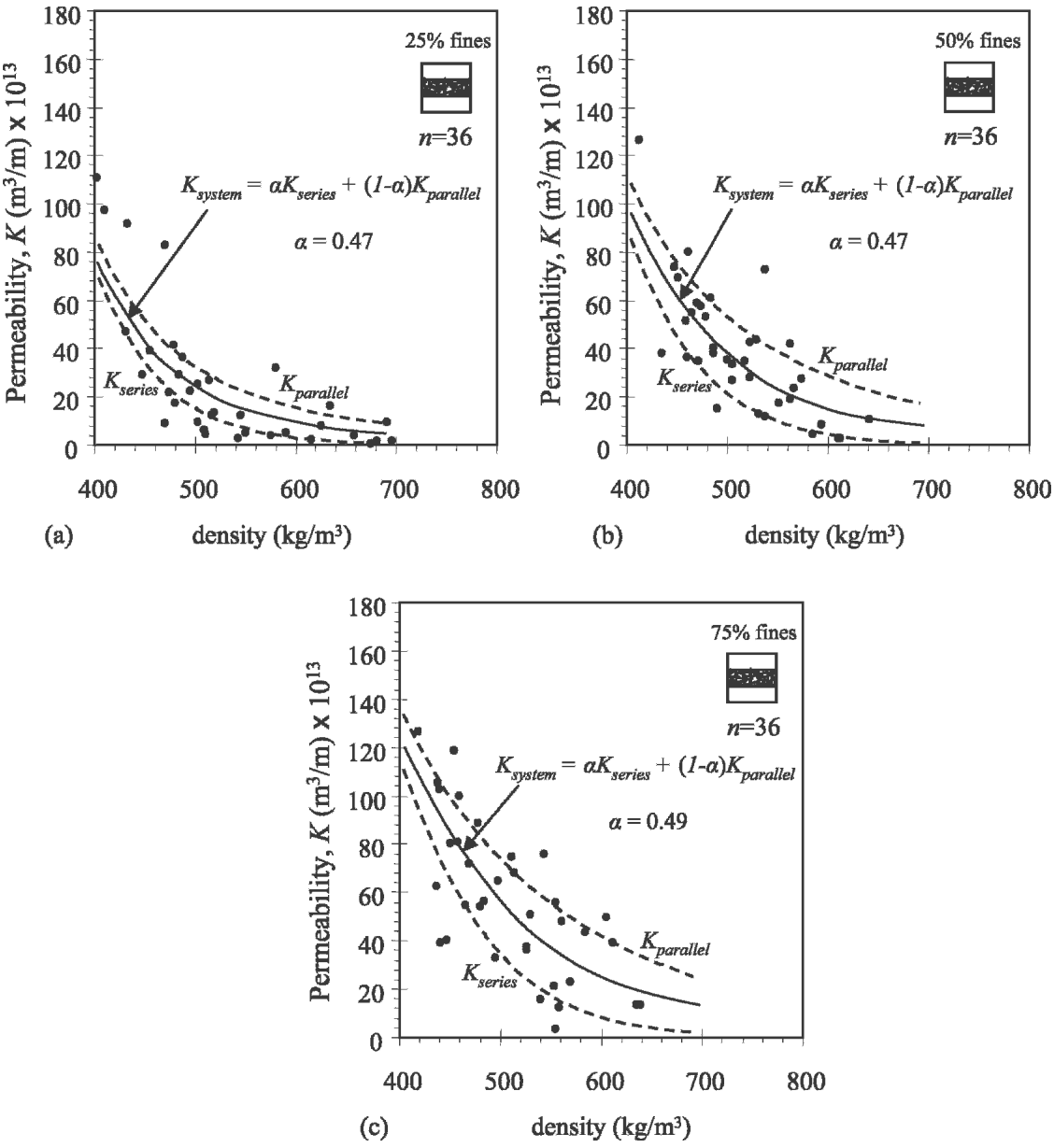

FIG. 4. Comparison of K_{core} values as a function of density for (*a*) 25% fines, (*b*) 50% fines, and (*c*) 100% fines. Predicted K_{system} at $\alpha = 0.48$ is shown in bold and the dashed lines indicate the permeability vs. density curves from the series and parallel models for each fines content.

Since the permeability of the parallel model is always higher than the series model, this suggests that the series configuration is the more common configuration in the core, which is evident from inspection of the transverse section through the pressed composite shown in Fig. 1a.

If α were to be rounded up to 0.5, then the system model may be simplified to the following:

$$K_{system} = \frac{K_{parallel} + K_{series}}{2} \tag{18}$$

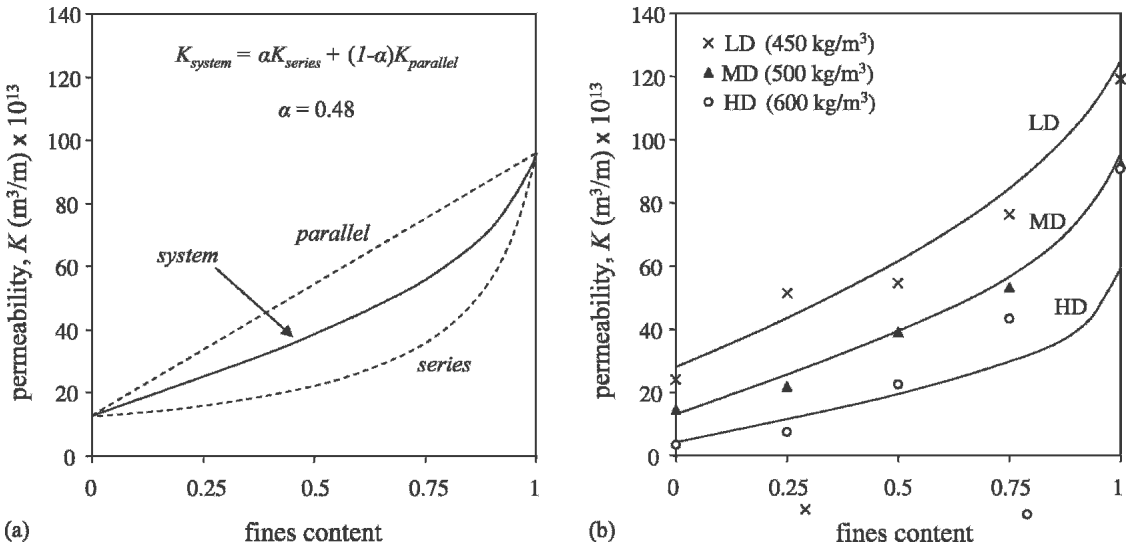

FIG. 5. The (*a*) predicted $K_{parallel}$, K_{series}, and K_{system} as functions of fines content for the core layer of OSB at 550 kg/m^3, and (*b*) mean K_{core} vs. fines content matched against model K_{system} for the low, medium, and high target density boards.

It is acknowledged that outside of the range of 25% to 75% fines content, there are no data for K_{core} from which to estimate α, and it cannot be assumed that α remains constant regardless of fines content. Since void volume and the connectivity of voids through the composite determine its permeability and are strongly affected by wood element geometry (Sekino 1994; Bolton and Humphrey 1994), it is expected that incorporating a larger number of shorter, narrower wood elements in a composite mat such as OSB might result in an increased number of shorter flow paths between elements that are in the parallel configuration. This would increase the ease with which vapor (and its latent heat) flow into and through the core during pressing. This was supported by the magnitude increases in permeability being greater above 50% fines content (Fig. 5b). The factors potentially influencing α, such as the proportions and distribution of strands and fines, mat formation technique, and composite density require further investigation.

Effect of density on model predictions and permeability data

The average K_{core} for each fines content and target density class is shown in Fig. 5b. The densities used, 450, 500 and 600 kg/m^3, are the mean densities of the core layer of boards in the low, medium, and high target density classes. The K_{system} predictions are well described by the permeability data for the low and medium target density boards, but deviate from the data in the case of the high-density boards at 75% and 100% fines content, whereby the model underestimates the permeability of the composite by around 35%. This discrepancy could have been caused by insufficient data for 100% fines in the higher density ranges. Note from Fig. 2a that there is only one data point for K_f above 600 kg/m^3 in density and it is therefore unknown whether this represents the true average permeability of 100% fines at this density level. It is also worth considering what happens to mat porosity at our different density levels and fines contents, as this may also help explain the observations, since mat porosity changes during compression were not factored into our model. According to Dai et al. (2005), mat porosity in OSB decreases sharply until mat density reaches about 500 kg/m^3, after which the rate of further decrease is low. However, when strand length and width are small (less than 30 mm and 10 mm in length and width, respectively); the inter-

strand mat porosity stays higher, which is consistent with the permeability here remaining high at high fines content even when the mat is highly compressed.

At the medium target density, the mat may have reached its maximum compression ratio. Further compression to the high target density likely resulted in little or no further change to void space. Another possible (but unconfirmed) reason for the discrepancy is that the mat may have undergone changes at high compression such as crushing of smaller, weaker wood elements that were unaccounted for in the permeability model. Such damage may have increased the interconnectivity of the void space, contributing to the observed increase in permeability.

Sensitivity analysis of the model

The sensitivity of the model, K_{system}, to ±15% change in the parameters M_f, K_s, K_f, ρ_s/ρ_f, and α is shown in Table 1, with a typical K_{system} response (in this case to M_f) shown in Fig. 6. The percentage change in K_{system} with increasing density is shown in Fig. 6b. The changes in K with up to ±15% change in M_f are symmetrical. From Table 1, the parallel model is more sensitive to changes in M_f than the series model since the term appears in the numerator of the parallel model and in the denominator of the series model. The sensitivity of K_{system} to M_f is greatest at high density, in accord with the observed trends in permeability in Fig. 5b. The permeability of the low density system was more sensitive to change in permeability of 100% strands, K_s, whereas the high density system was more sensitive to a change in the permeability of 100% fines, K_f. This is because K_s affects the series model while K_f affects the parallel model. The system became more sensitive to α as the density of the core increased; however, replotting K_{system} for $\alpha \pm 0.15\alpha$ showed minimal change in the permeability/density relationship. Table 1 indicates that K_{system} is most sensitive to the parameters M_f, K_f, and K_s, and a typical example of the magnitude of the response as a function of composite density is given in Fig. 6b. All of these parameters may be controllable by OSB plants, especially M_f. Permeability of the fines component may also be manipulated by modifying the size and shape of the fines through screening and/or subsequent refining of furnish.

Modeling the effects of mat structure and density on heat and mass transfer during hot-pressing must incorporate permeability both parallel *and* normal to the board plane over the density range during the press cycle. Less work has been done on in-plane permeability of wood composite mats and boards due to greater difficulty of measurement, but comparative data from Sokunbi (1978) showed that in-plane permeability of particleboard parallel to the plane was almost 60 times greater than transverse permeability normal to the board. The ratio of transverse to in-plane permeability in OSB mats is far lower than that for particle or fiber mats (Haas et al. 1998). It will be necessary to determine if a similar model can be applied to in-plane permeability of OSB containing different fines contents.

TABLE 1. *Variation (%) in predicted permeability of K_{system}, K_{series}, and $K_{parallel}$ to ±15% change in each parameter in a hypothetical composite containing 30% fines content and density of 520 kg/m^3.*

	K_{system}		K_{series}		$K_{parallel}$	
Parameters	−15%	+15%	−15%	+15%	−15%	+15%
M_f	−9.5	9.7	−5.2	5.9	−10.9	10.9
K_s	−5.9	5.8	−14.5	14.3	−2.9	2.9
K_f	−9.2	9.1	−0.7	0.5	−12.1	12.1
ρ_f/ρ_s	7.5	−6.0	4.5	−3.4	8.5	−6.9
α	6.4	−6.4	na	na	na	na

na = not applicable

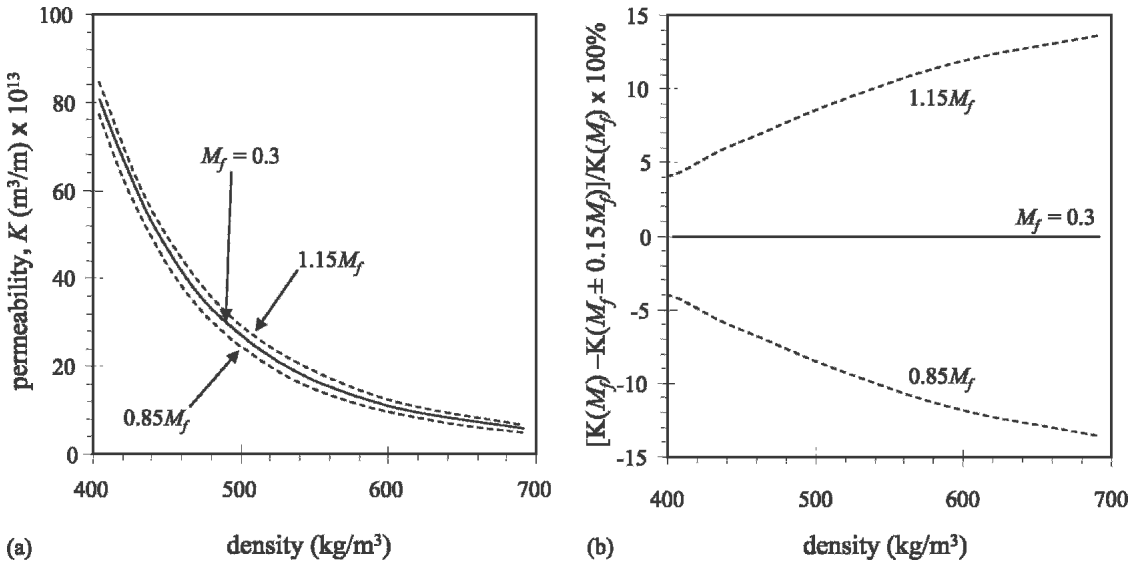

FIG. 6. Sensitivity of K_{system} to changing M_f, showing (*a*) K_{system} vs. density (solid line) and with ±15% change in M_f (dashed lines), and (*b*) percentage change in K_{system} with ±15% M_f for different densities.

CONCLUSIONS

1. The proposed rule of mixtures model for permeability, K_{system}, of an OSB core with fines content between 25% and 75% provided a good description of permeability data; K_{system} lies approximately midway between the permeability of parallel and series models.
2. $K_{parallel}$ is proportional to fines content, whereas K_{series} increases exponentially and is always lower than $K_{parallel}$ between 0 and 100% fines content.
3. The series coefficient, α, was essentially constant from 25% to 75% fines content; however, the true magnitude of α outside of 25 to 75% fines content is unknown. The model underestimated K_{core} for high density mats containing 75% fines or more by around 35%.
4. The model is sensitive to mass fraction of fines (M_f) and the permeability of 100% strands (K_s) and 100% fines (K_f).

ACKNOWLEDGMENTS

The authors wish to thank Ainsworth Lumber Co. Ltd. for providing furnish and information, Hexion Specialty Chemicals, Inc. for resin, and the Canadian National Science and Engineering Research Council (NSERC) for project funding. Permeability apparatus and guidance were kindly provided by Prof. S. Avramidis, Dept. of Wood Science, UBC.

REFERENCES

BOLTON, A. J., AND P. E. HUMPHREY. 1988. The hot pressing of dry-formed wood based composites. Part I: A review of the literature and some unpublished work. Holzforschung 48:95–100.

———, AND ———. 1994. The permeability of wood based composite materials I: A review of the literature and some unpublished work. Holzforschung 48:95–100.

BOWEN, M. E. 1970. Heat transfer in particleboard during pressing. PhD Thesis, Colorado State University, Fort Collins, CO.

DAI, C., AND C. YU. 2004. Heat and mass transfer in wood composite panels during hot pressing: Part I. A physical-mathematical model. Wood Fiber Sci. 36(4):585–597.

———, ———, AND P. HUBERT. 2000. Modeling vertical density profile in wood composites. Pages 220–226 *in* Proc. 5th Annual Pacific Rim Bio-Based Composites Symposium, Canberra, Australia.

———, ———, AND X. ZHOU. 2005. Heat and mass transfer in wood composite panels during hot pressing: Part II. Modeling void formation and mat permeability. Wood Fiber Sci. 37(2):2422–257.

GARCIA, P. J. 2002. Three dimensional heat and mass transfer during OSB hot pressing. PhD Thesis, The University of British Columbia. Vancouver, BC. 254 pp.

HAAS, G. VON. 1998. Investigations of the hot pressing of wood-composite mats: Compression behavior, permeability, temperature conductivity and sorption speed. PhD Dissertation, University of Hamburg, Germany.

———, A. STEFFEN, AND A. FRÜHWALD. 1998. Permeability of fiber, particle and strand mats to gas. Holz Roh-Werkst. 56:386–392.

HUBERT P., AND C. DAI. 1999. An object-oriented finite element processing model for oriented strand board wood composites. *In* Proc. 12th International Conference on Composite Materials (ICCM-12), Paris, France.

HUMPHREY, P. E., AND A. J. BOLTON. 1989. The hot pressing of dry-formed wood-based composites Part II: A simulation model of heat and moisture transfer, and typical results. Holzforschung 43(3):199–206.

———, AND H. THOEMEN. 2000. The continuous pressing of wood-based panels: An analytical simulation model, its validation and use. Pages 303–311 *in* Proc. 5th Annual Pacific Rim Bio-Based Composites Symposium, Canberra, Australia.

KAVVOURAS, P. K. 1977. Fundametal process variables in particleboard manufacture. PhD Thesis, University of Wales, Bangor, UK.

SEKINO, N. 1994. Humidity control efficiency of low-density particleboards for interior walls. III. Moisture sorption rates and moisture conductivities. Mokuzai Gakkaishi 40(4):519–526.

SOKUNBI, O. K. 1978. Aspects of particleboard permeability. MSc Thesis, University of Wales, Bangor, UK.

STRICKLER, M. D. 1959. Effect of press cycle and moisture content on properties of Douglas fir flakeboard. Forest Prod. J. 9(7):203–205.

ZOMBORI, G. B., F. A. KAMKE, AND L. T. WATSON. 2001. Simulation of the mat formation process. Wood Fiber Sci. 33(4):564–579.

———, ———, AND ———. 2003. Simulation of the internal conditions during the hot-pressing process. Wood Fiber Sci. 35(1):2–23.

———, ———, AND ———. 2004. Sensitivity analysis of internal mat environment during hot-pressing. Wood Sci. Technol. 35(1):2–23.